

Production of GeV-scale heavy neutral leptons in 3-body decays. Comparison with the PYTHIA approach

Volodymyr M. Gorkavenko, Yuliia R. Borysenkova
and Mariia S. Tsarenkova

*Faculty of Physics, Taras Shevchenko National University of Kyiv,
64, Volodymyrs'ka str., Kyiv 01601, Ukraine*

Abstract

Despite the undeniable success of the Standard Model of particle physics (SM), there are some phenomena that the SM can't explain. These phenomena indicate that the SM has to be modified. One of the possible ways to extend the SM is to introduce heavy neutral leptons (HNLs). To search for HNLs in intensity frontier experiments, one has to consider HNL production both in 2-body and 3-body decays of some mesons. We verified the possibility of using the parton level PYTHIA default matrix elements (without the form-factor formalism) to calculate HNL production in 3-body semileptonic decays of B and D mesons in the experimentally interesting mass range of the produced HNLs. We conclude that this approach is quite suitable for the estimation of the sensitivity region for HNLs in the intensity frontier experiments, provided one uses suitable parton level PYTHIA default matrix elements. Our study was driven by the usage of such an approximation by the SHiP collaboration. We conclude that in this case the parton level PYTHIA default matrix elements could have been chosen more appropriately.

Keywords: physics beyond the Standard Model, intensity frontier experiment, HNL.

1 Introduction

The Standard Model of particle physics (SM) [1, 2, 3] is a theory that describes with high precision the processes of electroweak and strong interactions with the participation of elementary particles. It is consistent up to a very high energy scale (perhaps up to the Planck scale) and it is verified in numerous accelerator experiments up to energy ~ 15 TeV. However, the SM fails to explain some phenomena such as massiveness of neutrinos (see e.g. [4, 5]), dark matter (for reviews see e.g. [6, 7, 8]), dark energy [9], baryon asymmetry of the Universe [10], etc. Therefore, the SM is an incomplete theory and it requires an extension. One has to suggest the existence of "hidden" sectors with particles of new physics.

It turns out that the mentioned SM problems can be theoretically solved by extending the SM by new particles that can be either heavy or light. Indeed, neutrino oscillations and the smallness of the active neutrino masses can be explained with the help of new

particles with sub-eV mass as well as with the help of heavy particles of the GUT scale, see e.g. [11]. The same may be said about the baryon asymmetry of the Universe and dark matter problems: physics at very different scales can be responsible for them, see e.g. [12].

So, two possible answers can be formulated to the question "why do we not observe particles of new physics in experiments?" The first answer is the following. The new particles are very heavy and can't be produced in modern accelerators like the LHC. To detect them one has to build more powerful and more expensive accelerators (we need energy frontier experiments). However, there is another possibility. The particles of new physics can be light (with a mass below or of the order of the electroweak scale) that feebly interact with the SM particles. The last case is very interesting for the experimental search for new physics right now, see e.g. [13]. To search for rare interactions of feebly interacting hypothetical particles, the intensity frontier experiments are needed. These experiments aim to create high-intensity particle beams and use large detectors [14]. Several such intensity frontier experiments have been proposed in recent years: DUNE [15], NA62 [16, 17, 18], SHiP [19, 20], etc.

We do not know what are the properties of the new particles. They can be new scalars, pseudoscalars, vectors or fermions, see [19, 21] for a review. Each of these options has to be tested in experiments. From a theoretical point of view, there are three possible choices of the new renormalized Lagrangian of the interaction of new particles with the SM particles. These interactions are called portals. There are scalar (e.g. [22, 23, 24]), vector (e.g. [25, 26, 27]) and heavy neutral leptons renormalized portals. It means the new interaction can be observed at any energy scale, including that below the EW scale. There are also other portals of high-dimensional operators such as the portal of pseudoscalar particles (axion-like particles), see e.g. [28, 29, 30] and [31] for a review, or Chern-Simons like (parity odd) interaction of electroweak gauge bosons with a new vector field (e.g. [32, 33]). The lower the energy scale is, the less important these interactions will be.

In this paper, we consider extending the SM by neutrino singlets with right chirality, which extremely faintly interact with the SM particles. Such right-handed neutrinos are called sterile neutrinos or heavy neutral leptons (HNLs).

Interest in the HNL modification of the SM is conditioned by the model's ability to explain the smallness of active neutrino masses (due to large values of the sterile neutrino masses M_I or small values of Yukawa elements $F_{\alpha I}$) and to describe the generation of the matter-antimatter asymmetry of the Universe due to CP violation in the model [34]. It was shown that Majorana masses of HNLs can be GeV scale [35, 36, 37] to explain baryon asymmetry of the Universe.

In 2005 the Neutrino Minimal Standard Model (νMSM) model was proposed [36, 38]. In this model, the SM is extended by three right-handed neutrinos (heavy neutral leptons) with masses smaller than the electroweak scale. It was shown that 18 new parameters of the model can be chosen in such a way as to simultaneously solve problems of neutrino oscillations, baryon asymmetry in the Universe, and dark matter. In this case, the νMSM model requires the existence of two right-handed neutrinos with practically the same masses ($\gtrsim 100$ MeV) and one right-handed neutrino with a relatively small mass in the keV region, see [39] for a review. The lightest right-handed neutrino is a long-lived particle, a dark matter candidate. In 2014 the possible manifestation of the lightest right-handed neutrino with mass 7 keV was found in X-ray spectra of the Andromeda galaxy and the Perseus galaxy cluster [40, 41].

That is why the HNL extension of the SM attracts a lot of attention and interest.

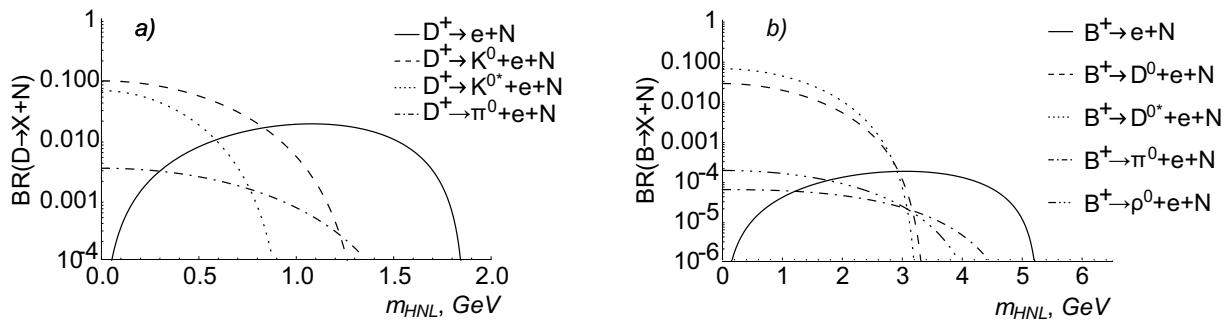


Figure 1: Dominant branching ratios of HNL production from charged D (figure *a*) and B (figure *b*) mesons, see [43] for details. Here $U_e = 1$, $U_\mu = U_\tau = 0$.

This modification of the SM is especially interesting for GeV-scale HNLs that can be in principle detected in the intensity frontier experiments [14, 19].

A model-independent phenomenological approach is used in the experimental search for HNLs, assuming the existence of only one HNL and considering that the other HNLs do not affect the analysis. For simplicity of analysis, restrictions are imposed on only two free parameters of the model: Majorana mass of the appropriate HNL (m_N) and the mixing angle of the interaction of this HNL with only one active neutrino of flavour α (U_α). While it is usually assumed that the mixing angles of interaction with other active neutrinos are zero.

It should be noted that the results of previous numerous experiments almost completely closed the region for HNLs with masses below the mass of kaon, see [19, 42] for details. Therefore, HNLs with mass $m_N \gtrsim 0.5$ GeV are of interest to us. The phenomenology of GeV-scale HNLs was considered e.g. in [43]. A recent computation of the sensitivity region for HNL search in the SHiP experiment was performed in [44].

If we consider the most important production channels of HNLs in the fixed target intensity frontier experiments (such as NA62, SHiP or DUNE), we see that they are the semileptonic decays of D , D_s mesons, B , B_s , B_c mesons and decays of τ leptons, see [43]. It should be noted that an essential contribution to HNL production is given by 3-body decays of the mentioned particles, see figure 1, where we present branchings for decays of D and B mesons as an example. Branchings for decays of other mesons can be found in [43].

Taking into account that the number of the produced D mesons is sufficiently greater than the number of the produced B mesons in proton-target collisions (e.g. $\sim 10^{17}$ and $\sim 10^{13}$ correspondingly for 5 years of SHiP experiment operation [43]), it is obvious that HNLs production from B mesons decay can be neglected for HNLs with masses $m_N \lesssim 2$ GeV.

So, 3-body decays of mesons with τ leptons in the final state are either forbidden (for the decays of D mesons) or ineffective (for the decays of B mesons). We will denote the final states of charged leptons as $\ell = e, \mu$.

In the SHiP collaboration paper [44] computation of the 3-body semileptonic decay contributions ($h \rightarrow h' + \ell + N$) for the formation of the sensitivity region for HNLs was based on PYTHIA 8. PYTHIA is a general purpose collision event generator [45], that can be modified to embody new simulations with an arbitrarily good approximation in principle. However, the 3-body decay contributions to the sensitivity region built in [44] were computed with use of the parton level PYTHIA default matrix elements

without additional tuning. This can be clearly seen by looking at their program code¹. It motivated us to verify the accuracy of this approach.

The fact is that for the description of the semileptonic decays of D mesons PYTHIA uses a default matrix element

$$|M_{fi}|^2 = (p_h p_\ell)(p_\nu p_{h'}) \quad (1)$$

and for description of the semileptonic decays of B mesons PYTHIA uses a default matrix element

$$|M_{fi}|^2 = (p_h p_\nu)(p_\ell p_{h'}). \quad (2)$$

Explicit form of these matrix elements is given in the PYTHIA 6.4 manual [46]. The current version, PYTHIA 8, uses the same matrix elements without change. Our further computations are valid for PYTHIA 6 as well as for PYTHIA 8.

However, for accurate consideration we need to use at least form-factors of meson transitions. In this paper, we analyze the relevancy of the usage of the parton level default PYTHIA matrix elements in the SHiP collaboration paper [44] for the computation of the contributions of the 3-body decays of B and D mesons to the sensitivity region.

As it was pointed out in [19] HNLs can be produced in τ lepton decays and these decays are important in case of dominant mixing with the τ flavour. The main 3-body decay channels of τ leptons are decays into elementary particles $\tau \rightarrow N \ell_\alpha \bar{\nu}_\alpha$ and $\tau \rightarrow \nu_\tau \ell_\alpha N$, where $\alpha = e, \mu$. In contrast to meson decays, which must be described using the form-factor formalism, these decays can be directly described by the PYTHIA formalism.

The paper is organized in the following way. In section 2 we consider a general formalism of the neutrino modification to the Standard Model. In section 3 we formulate a general strategy to get the domain of parameters that allows hidden particles to be detected in the intensity frontier experiments. In section 4 we get the general definition of a probability density function (PDF) for the production of particles with a certain value of energy in 3-body decays. In section 5 and section 6 we present the exact matrix elements for the 3-body decays of mesons. In section 7 we compare PDFs for HNL production in 3-body decays of mesons (in the own reference frame of the mesons) computed using the parton level PYTHIA default matrix elements and the exact ones. In section 8 we derive the energy and polar angle distribution functions of the produced HNLs in the laboratory reference frame. In section 9 we find the probability of a produced HNL to fall on the detector. In section 10 we estimate the probability of a produced HNL to decay inside the vacuum tank before the detector. Finally, the results are summarized in section 11. Useful kinematic relations for HNLs in the different reference frames are outlined in appendix A.

2 Neutrino modification of the SM. Heavy Neutral Leptons

Renormalized interaction of the right-handed neutrinos with the SM particles (HNL portal) is similar to the Yukawa interaction of left-handed quark doublets with singlets of the right-handed quarks in the SM, namely:

$$\mathcal{L}_{int} = - \left(F_{\alpha I} \bar{L}_\alpha \tilde{H} N_I + \text{h.c.} \right), \quad (3)$$

¹The calculations of the SHiP collaboration were carried out with the use of the FairShip software framework. The program code is in open access, see <https://github.com/ShipSoft/FairShip>

where $\alpha = e, \mu, \tau$, the index I is from 1 to the full number of the sterile neutrinos (n), L_α – the doublet of the leptons of α -generation, N_I – a right-handed sterile neutrino, $F_{\alpha I}$ – a new matrix of dimensionless Yukawa couplings, $\tilde{H} = i\sigma_2 H^*$.

Conditions of invariance of the Lagrangian (3) to the transformations of the gauge groups of the SM demand the corresponding charges of the sterile neutrinos to be zero. Therefore, sterile neutrinos are not charged relative to the gauge groups of the SM, which justifies their name.

After the electroweak symmetry breaking, Lagrangian (3) in the unitary gauge looks as follows:

$$\mathcal{L}_{int} = - (M_{\alpha I}^D \bar{\nu}_\alpha N_I + \text{h.c.}), \quad M_{\alpha I}^D = \frac{v}{\sqrt{2}} F_{\alpha I}, \quad (4)$$

where $v \approx 246$ GeV is the vacuum expectation value of the Higgs field, $M_{\alpha I}^D$ – Dirac mass terms.

Considering sterile neutrinos as neutral Majorana particles, we can write the full Lagrangian of the modified neutrino sector of the SM in the form

$$\mathcal{L}_{\nu, N} = i\bar{\nu}_k \not{\partial} \nu_k + i\bar{N}_I \not{\partial} N_I - \left(M_{\alpha I}^D \bar{\nu}_\alpha N_I + \frac{M_I}{2} \bar{N}_I^c N_I + \text{h.c.} \right), \quad (5)$$

where M_I is the Majorana mass of I th sterile neutrino. Imposing the condition $M_{I\alpha}^D/M_I \ll 1$, one can perform the diagonalization of the neutrino mass matrix, see e.g. [11, 47], and get the mass matrix of the active neutrinos

$$(M_\nu^{active})_{\alpha\beta} = - \sum_{I=1}^n \frac{M_{I\alpha}^D M_{I\beta}^D}{M_I}. \quad (6)$$

The mass matrix for the sterile neutrinos will remain almost unchanged. This mechanism is known as the seesaw mechanism¹, see e.g. [54, 55].

As a result of the neutrino states mixture, the active neutrino states become superposition of the mass states of the active and sterile neutrinos

$$\nu_L = \left(1 - \frac{1}{2} U^+ U \right) V_1 \nu_{mL} + U^+ V_2 N^c, \quad (7)$$

where $U_{I\alpha} = M_{I\alpha}^D/M_I$ ($U = M^{-1}M^D$) is a so-called mixing angle ($U_{I\alpha} \ll 1$), V_1 – a unitary matrix for diagonalization of the active neutrino mass matrix, V_2 – a unitary matrix for diagonalization of the sterile neutrino mass matrix (it can be taken as a unit matrix in our case). It means that sterile neutrinos interact with the SM particles similarly to active neutrinos:

$$\mathcal{L}_{int} = - \frac{g}{2\sqrt{2}} W_\mu^+ \sum_{I,\alpha} \bar{N}_I^c U_{I\alpha} \gamma^\mu (1 - \gamma_5) \ell_\alpha^- - \frac{g}{4 \cos \theta_W} Z_\mu \sum_{I,\alpha} \bar{N}_I^c U_{I\alpha} \gamma^\mu (1 - \gamma_5) \nu_\alpha + \text{h.c.} \quad (8)$$

It should be noted that the extension of the SM by HNLs gives an additional source of CP-symmetry violation in the theory, see e.g. [56].

¹This mechanism is called Type-I seesaw mechanism because there are other ways to explain small neutrino masses, see e.g. [11, 48]. In the Type-II seesaw mechanism an extra SU(2) triplet scalar is introduced [49, 50, 51, 52], in the type-III seesaw mechanism an extra fermion in the adjoint of SU(2) is added to the model [53].

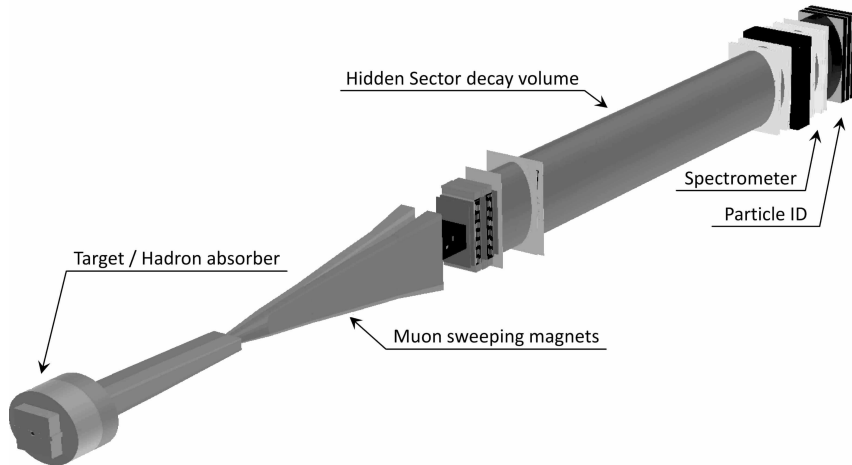


Figure 2: General scheme of the SHiP facility.

3 General strategy

At first, let us remind the general principles of the intensity frontier experiments operation on the example of an intended experiment SHiP [57], see figure 2. A beam line from the CERN SPS accelerator will transmit 400 GeV protons at the SHiP. A proton beam will strike in a Molybdenum and Tungsten fixed target at a center-of-mass energy $E_{CM} \approx 27$ GeV. A great number of light SM particles and hadrons will be produced under such collisions. Hidden particles are expected to be predominantly produced in the decays of the produced hadrons.

The main concept of the SHiP functioning is the following. Almost all the produced SM particles should be either trapped by an absorber or deflected in a magnetic field (muons). Remaining events with the SM particles can be rejected using specially developed cuts. If hidden particles decay into SM particles inside the decay volume, the latter will be detected. It will mean the existence of hidden particles.

We can estimate the number of hidden particles that can be detected as

$$N_{det} = N_{BSM} \cdot \epsilon_{tot} \cdot P_{decay}. \quad (9)$$

This relation allows us to find a range of parameters (m_N, θ_α) , when HNLs can be detected. It is a region where $N_{det} \geq N_{det}^{thr}$. Value N_{det}^{thr} is the threshold number of the detected particles when we can affirm the discovery of HNLs. It depends on the characteristics of the experiment facilities and the background level.

Let us explain the meaning of the constituent factors in (9). Factor N_{BSM} is the number of hidden particles produced during all the time of the SHiP experiment operation. Factor ϵ_{tot} is the product of the following factors $\epsilon_{geom} \cdot Br_{vis} \cdot \epsilon_{det}$, where ϵ_{geom} is the probability of a produced HNL to move towards the detector, ϵ_{det} is the probability of the detector to register visible particles, Br_{vis} is the branching of HNL decay into channels, visible for the detectors. Factor P_{decay} is the probability of a produced HNL to decay in the volume of the vacuum tank before the detectors.

Therefore, to validate the accuracy of the computation with use of the parton level PYTHIA default matrix elements of the contribution of the produced in the 3-body decays HNLs to the sensitivity region we have to consider only two factors in (9), namely ϵ_{geom} and P_{decay} .

The probability for the produced HNLs to move towards the detector (ϵ_{geom}) can be easily found if we know the distribution function of these particles. The probability of the HNLs to decay inside the vacuum tank before the detector is

$$P_{decay} = e^{-\frac{L\Gamma}{\gamma\beta}} - e^{-\frac{(L+\Delta L)\Gamma}{\gamma\beta}}, \quad (10)$$

where L is the distance from the target to the vacuum tank, ΔL – the length of the vacuum tank, γ is the Lorentz factor, β – the velocity of the particle and Γ – the decay width of HNLs. Thus, P_{decay} depends on the energy distribution function of HNLs, HNL's lifetime, geometry of the experiment, and the coupling constant.

Therefore, to compute both ϵ_{geom} and P_{decay} we need the energy-angle distribution functions of the produced HNLs. One can easily get these functions in the rest frame of the initial meson. Using the energy-angle distribution of the initial mesons, we can get the distribution functions of HNLs in the laboratory reference frame. We assume that in the initial meson's rest frame the production of HNLs is isotropic.

4 Probability density function for particles produced in a 3-body decay

Let us consider a 3-body decay $A \rightarrow B + C + N$, where A, B, C are some particles (with masses m_A, m_B, m_C) and N is a sterile neutrino with mass m_N .

If the decaying particle (A) is a scalar (or we average over its spin states), the differential decay width of the 3-body decay in the rest frame of the A particle is defined as, see e.g. [58],

$$d\Gamma = \frac{|M_{fi}|^2}{8m_A(2\pi)^3} dE_N dE_B. \quad (11)$$

The full partial decay width for this channel is given as

$$\Gamma(A \rightarrow BCN) = \int_{E_N^{min}}^{E_N^{max}} dE_N \int_{E_B^{min}(E_N)}^{E_B^{max}(E_N)} dE_B \frac{|M_{fi}|^2}{8m_A(2\pi)^3}, \quad (12)$$

where the boundaries of integration can be found from condition

$$E_N^{2\ max/min} = m_N^2 + \vec{p}_N^{2\ max/min} = m_N^2 + \vec{p}_B^2 + \vec{p}_C^2 \pm 2|\vec{p}_B||\vec{p}_C|, \quad (13)$$

that can be rewritten as the solution of equation

$$E_N^{2\ max/min} = m_N^2 + E_B^2 - m_B^2 + (m_A - E_N - E_B)^2 - m_C^2 \pm 2\sqrt{(E_B^2 - m_B^2)((m_A - E_N - E_B)^2 - m_C^2)}, \quad (14)$$

namely

$$E_B^{max/min}(E_N) = \frac{(m_A - E_N)(w^2 + m_B^2 - m_C^2)}{2w^2} \pm \sqrt{E_N^2 - m_N^2} \frac{\sqrt{\lambda(w^2, m_B^2, m_C^2)}}{2w^2}, \quad (15)$$

where $w^2 = m_A^2 + m_N^2 - 2E_N m_A$ and $\lambda(x, y, z) = x^2 + y^2 + z^2 - 2xy - 2yz - 2zx$ is the Källén function [59].

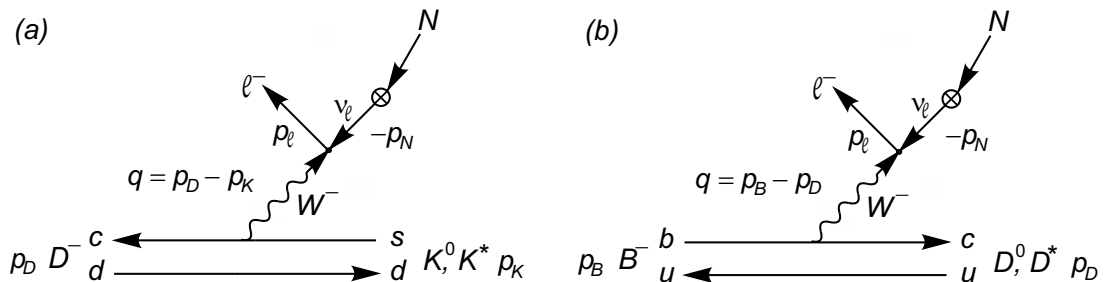


Figure 3: Diagram of the semileptonic decays: (a) – decay of pseudoscalar meson D^- into pseudoscalar meson K^0 or vector meson $K^*(892)$, (b) – decay of pseudoscalar meson B^- into pseudoscalar meson D^0 or vector meson $D^*(2007)^0$.

As one can see, two functions $E_{B \text{ max/min}}(E_N)$ in (15) define the upper and lower boundaries of the region with the allowed values of energy. These functions coincide at the minimal and maximum values of the energy E_N that can be found from the condition for the changing sign term being zero. We get

$$E_N^{\min} = m_N, \quad E_N^{\max} = \frac{m_A^2 + m_N^2 - (m_B + m_C)^2}{2m_A}. \quad (16)$$

Taking into account (12), we get the probability density function (PDF) for the production of HNLs with a certain value of energy (E_N) in the form

$$pdf(E_N) = \frac{1}{\Gamma(A \rightarrow BCN)} \int_{E_B^{\min}(E_N)}^{E_B^{\max}(E_N)} dE_B \frac{|M_{fi}|^2}{8m_A(2\pi)^3}. \quad (17)$$

5 HNL production in semileptonic decays of B and D mesons into pseudoscalar mesons

Decay of an electrically charged pseudoscalar meson h into an electrically neutral pseudoscalar meson h' , a charged lepton and an HNL ($h \rightarrow h' + \ell + N$) is derived by weak interaction, see figure 3. The amplitude of the reaction is

$$M_{fi} = \theta_\alpha \frac{G_F}{\sqrt{2}} V_{ij}^* \bar{\ell}_\alpha \gamma^\nu (1 - \gamma^5) N \langle h'(p') | \bar{Q}_i \gamma_\nu (1 - \gamma^5) Q_j | h(p) \rangle, \quad (18)$$

where averaging over the axial quark current gives zero, but averaging over vector quark current can be presented as

$$\mathcal{W}_\nu = \langle h'(p') | \bar{Q}_i \gamma_\nu Q_j | h(p) \rangle = \left[(p+p')_\nu - \frac{m_h^2 - m_{h'}^2}{q^2} q_\nu \right] f_+^{hh'}(q^2) + \frac{m_h^2 - m_{h'}^2}{q^2} q_\nu f_0^{hh'}(q^2), \quad (19)$$

where $f_+^{hh'}(q^2)$ and $f_0^{hh'}(q^2)$ are the form-factors for hh' transitions.

For $|M_{fi}|^2$ summarized over the helicities of the final particles, we have

$$\overline{|M_{fi}|^2} = 4\theta_\alpha^2 G_F^2 |V_{ij}|^2 [2(m_h^2 - m_{h'}^2) f_0^{hh'}(q^2) (k\mathcal{W}) - 2(k\mathcal{W})^2 - (qk)\mathcal{W}^2 + m_N^2 \mathcal{W}^2], \quad (20)$$

where m_h , $m_{h'}$ are the masses of the corresponding mesons, m_N – the mass of the sterile neutrino.

Table 1: Best fit parameters for the form-factors (21) of $B \rightarrow D$ transitions [61].

f	M_{pole} (GeV)	a_0	a_1	a_2
f_+^{BD}	∞	0.909	-7.11	66
f_0^{BD}	∞	0.794	-2.45	33

Table 2: Best fit parameters for the form-factors (25) of $D \rightarrow K$ transitions [63].

f	$f(0)$	c	P (GeV $^{-2}$)
f_+^{DK}	0.7647	0.066	0.224
f_0^{DK}	0.7647	2.084	0

For consideration of reaction $B^\pm \rightarrow D^0 + \ell^\pm + N$ we use a popular parametrization for form-factors of mesons, namely the Bourely-Caprini-Lellouch (BCL) parametrization [60] that takes into account the analytic properties of the form-factors (see e.g. [61, 62]),

$$f(q^2) = \frac{1}{1 - q^2/M_{\text{pole}}^2} \sum_{n=0}^{N-1} a_n \left[(z(q^2))^n - (-1)^{n-N} \frac{n}{N} (z(q^2))^N \right], \quad (21)$$

where function $z(q^2)$ is defined via

$$z(q^2) \equiv \frac{\sqrt{t_+ - q^2} - \sqrt{t_+ - t_0}}{\sqrt{t_+ - q^2} + \sqrt{t_+ - t_0}} \quad (22)$$

with

$$t_+ = (m_h + m_{h'})^2. \quad (23)$$

The choice of t_0 and the pole mass M_{pole} varies from group to group that performs the analysis. In this work we follow the FLAG collaboration [61] and take

$$t_0 = (m_h + m_{h'}) (\sqrt{m_h} - \sqrt{m_{h'}})^2. \quad (24)$$

The coefficients a_n^+ and a_n^0 are then fitted to the experimental data or lattice results. Their best fit parameter values are given in table 1.

For consideration of reaction $D^\pm \rightarrow K^0 + \ell^\pm + N$ we use the parametrization for form-factors of mesons given in [63]:

$$f(q^2) = \frac{f(0) - c(z(q^2) - z_0) \left(1 + \frac{z(q^2) + z_0}{2}\right)}{1 - Pq^2}, \quad (25)$$

where $z(q^2)$ is defined by (22) and $z_0 = z(0)$. The best fit parameter values are given in table 2.

6 HNL production in semileptonic decays of B and D mesons into vector mesons

Let us consider production of HNLs in semileptonic decays of B and D mesons into vector mesons, namely $B^\pm \rightarrow D^*(2007)^0 + \ell^\pm + N$ and $D^\pm \rightarrow K^*(892) + \ell^\pm + N$.

Decay of an electrically charged pseudoscalar meson h into an electrically neutral vector meson h'_V , a charged lepton and an HNL ($h \rightarrow h'_V + \ell + N$) is derived by weak interaction, see figure 3. The amplitude of the reaction is similar to (18), where there is contribution from both the vector and the axial parts of the quark current $\bar{Q}_i \gamma_\nu (1 - \gamma^5) Q_j = V_\nu - A_\nu$, see [43]:

$$\langle h'_V(\epsilon, p') | V_\mu | h(p) \rangle = ig(q^2) \varepsilon_{\mu\alpha\sigma\rho} \epsilon^{*\alpha} (p+p')^\sigma (p-p')^\rho = i2g(q^2) \varepsilon_{\mu\alpha\sigma\rho} \epsilon^{*\alpha} p'^\sigma p^\rho = iV_\mu, \quad (26)$$

$$\langle h'_V(\epsilon, p') | A_\mu | h(p) \rangle = f(q^2) \epsilon_\mu^* + a_+(q^2) (\epsilon^* \cdot p) (p+p')_\mu + a_-(q^2) (\epsilon^* \cdot p) (p-p')_\mu = \mathbb{A}_\mu, \quad (27)$$

and ϵ_μ is the polarization vector of the vector meson.

For $|M_{fi}|^2$ summarized over the helicities and polarization states of the final particles, we have

$$\overline{|M_{fi}|^2} = 4\theta_\alpha^2 G_F^2 |V_{ij}|^2 \sum_\lambda R^{\mu\nu} [\mathbb{V}_\nu \mathbb{V}_\mu^* + \mathbb{A}_\nu \mathbb{A}_\mu^* + i(\mathbb{A}_\nu \mathbb{V}_\mu^* - \mathbb{V}_\nu \mathbb{A}_\mu^*)], \quad (28)$$

where λ is the polarization state of the vector meson and

$$R^{\mu\nu} = (q^\nu - k^\nu) k^\mu - (qk) g^{\nu\mu} + m_N^2 g^{\nu\mu} + (q^\mu - k^\mu) k^\nu - iq_i k_j \varepsilon^{ij\nu\mu}. \quad (29)$$

Summation over the polarization states of the vector meson can be performed directly using the relation

$$\sum_\lambda \varepsilon_\alpha^*(p') \varepsilon_\beta(p') = - \left(g_{\alpha\beta} - \frac{p'_\alpha p'_\beta}{m_{h'_V}^2} \right). \quad (30)$$

We get

$$\sum_\lambda R^{\mu\nu} \mathbb{V}_\nu \mathbb{V}_\mu^* = 8g^2(q^2) \{ m_B^2 [(p'k)^2 - m_D^2(qk)] + m_D^2(pk)^2 + (pp') [-2(p'k)(pk) + (pp')(qk)] \}, \quad (31)$$

$$\sum_\lambda R^{\mu\nu} i(\mathbb{A}_\nu \mathbb{V}_\mu^* - \mathbb{V}_\nu \mathbb{A}_\mu^*) = 8g(q^2) f(q^2) [m_B^2(p'k) + m_D^2(pk) - (p'k + pk)(pp')], \quad (32)$$

$$\begin{aligned} \sum_\lambda R^{\mu\nu} \mathbb{A}_\mu \mathbb{A}_\nu^* &= -R^2(m_N^2 - qk) \left(m_B^2 - \frac{(pp')^2}{m_D^2} \right) + \frac{2(kR)(kR - qR)}{m_D^2} + \\ &+ 2f(q^2) [(kQ)(qR) + (kR)(qQ - 2kQ) + (RQ)(m_N^2 - qk)] + \\ &+ f^2(q^2) \left(\frac{2(p'k)(p'p - p'k)}{m_D^2} - m_N^2 + qk - 2p'k \right), \end{aligned} \quad (33)$$

where

$$R_\mu = a_+(q^2)(p+p')_\mu + a_-(q^2)(p-p')_\mu, \quad Q_\nu = \frac{(pp')}{m_D^2} p'_\nu - p_\nu. \quad (34)$$

Form-factors $f(q^2)$, $g(q^2)$, $a_\pm(q^2)$ can be found from the dimensionless linear combinations [64, 65, 66]:

$$V^{hh'}(q^2) = (m_h + m_{h'}) g^{hh'}(q^2), \quad (35)$$

$$A_0^{hh'}(q^2) = \frac{1}{2m_{h'}} \left(f^{hh'}(q^2) + q^2 a_-^{hh'}(q^2) + (m_h^2 - m_{h'}^2) a_+^{hh'}(q^2) \right), \quad (36)$$

$$A_1^{hh'}(q^2) = \frac{f^{hh'}(q^2)}{m_h + m_{h'}}, \quad (37)$$

$$A_2^{hh'}(q^2) = -(m_h + m_{h'}) a_+^{hh'}(q^2), \quad (38)$$

Table 3: First part of the table with parameters of form-factors (39-41) of B and D mesons decays into vector mesons [64, 65, 66].

h, h'	$f_V^{hh'}$	$f_{A_0}^{hh'}$	$f_{A_1}^{hh'}$	$f_{A_2}^{hh'}$	$\sigma_V^{hh'}$	$\sigma_{A_0}^{hh'}$	$\sigma_{A_1}^{hh'}$	$\sigma_{A_2}^{hh'}$
D, K^*	1.03	0.76	0.66	0.49	0.27	0.17	0.30	0.67
B, D^*	0.76	0.69	0.66	0.62	0.57	0.59	0.78	1.40

Table 4: Second part of the table with parameters of form-factors (39-41) of B and D mesons decays into vector mesons [64, 65, 66].

h, h'	$\xi_V^{hh'}$	$\xi_{A_0}^{hh'}$	$\xi_{A_1}^{hh'}$	$\xi_{A_2}^{hh'}$	M_P^h (GeV)	M_V^h (GeV)
D, K^*	0	0	0.20	0.16	m_{D_s}	$m_{D_s^*}$
B, D^*	0	0	0	0.41	m_{B_c}	$m_{B_c^*}$

that can be parameterized as

$$V^{hh'}(q^2) = \frac{f_V^{hh'}}{1 - q^2/(M_V^h)^2[1 - \sigma_V^{hh'}q^2/(M_V^h)^2 - \xi_V^{hh'}q^4/(M_V^h)^4]}, \quad (39)$$

$$A_0^{hh'}(q^2) = \frac{f_{A_0}^{hh'}}{1 - q^2/(M_P^h)^2[1 - \sigma_{A_0}^{hh'}q^2/(M_V^h)^2 - \xi_{A_0}^{hh'}q^4/(M_V^h)^4]}, \quad (40)$$

$$A_{1/2}^{hh'}(q^2) = \frac{f_{A_{1/2}}^{hh'}}{1 - \sigma_{A_{1/2}}^{hh'}q^2/(M_V^h)^2 - \xi_{A_{1/2}}^{hh'}q^4/(M_V^h)^4}. \quad (41)$$

The best fit values of parameters are given in papers [64, 65, 66]. The parameters f and σ are given in table 3. The parameters ξ and the pole masses M_V, M_P are given in table 4, where $m_{D_s} = 1.969$, $m_{D_s^*} = 2.112$, $m_{B_c} = 6.275$, $m_{B_c^*} = 6.331$. The mass for B_c^* was taken from theoretical prediction [67].

7 PDF for HNLs produced in 3-body decays

In this paper, we consider HNL production in 3-body decays of pseudoscalar B and D mesons into other pseudoscalar mesons, namely $B^\pm \rightarrow D^0 + \ell^\pm + N$ and $D^\pm \rightarrow K^0 + \ell^\pm + N$. Also we consider HNL production in 3-body decays of pseudoscalar B and D mesons into vector mesons, namely $B^\pm \rightarrow D^*(2007)^0 + \ell^\pm + N$ and $D^\pm \rightarrow K^*(892) + \ell^\pm + N$. Two cases of leptons ($\ell = e, \mu$) in the final states are practically indistinguishable because of the small masses of electron and muon as compared with the masses of mesons in the reactions.

Let us compare the probability density function in the own frame of the initial meson for production of HNLs with a certain energy (E_N) computed with the help of relation (17) for the exact matrix elements (see section 5 and section 6) and for the parton level PYTHIA default matrix elements, see (1), (2).

We see that the PDF computed exactly for the reaction of HNL production in the decay of the pseudoscalar meson B into the pseudoscalar meson D^0 is in good agreement with the PDF computed with the PYTHIA default matrix element for the decay of B mesons (2), see figure 4. But the PDF computed exactly for the reaction of the B meson decay into a vector meson $B^\pm \rightarrow D^*(2007)^0 + \ell^\pm + N$ is in good agreement not with the

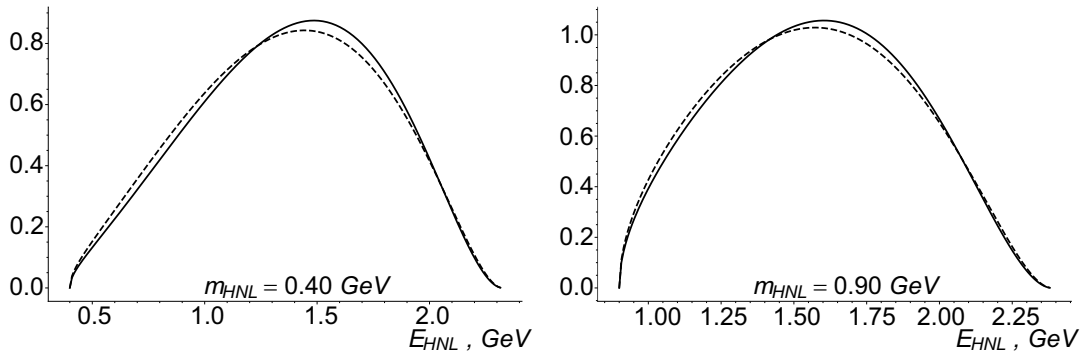


Figure 4: Probability density functions for the energy of HNLs (in the rest frame of the initial meson) produced in the reaction $B^\pm \rightarrow D^0 + \ell^\pm + N$ computed exactly (solid line) and with the PYTHIA default matrix element for decays of B meson (2) (dashed line).

PDF computed with the PYTHIA default matrix element for decays of B mesons (2), but with the PDF computed with the PYTHIA default matrix element for decays of D mesons (1), see figure 5.

We see that the PDF computed exactly for the reaction of HNL production in the decay of the pseudoscalar meson D into the pseudoscalar meson K^0 is in good agreement not with the PDF computed with the PYTHIA default matrix element of the D meson decays (1), but with the PDF computed with the PYTHIA default matrix element for decays of B mesons (2), see figure 6. But the PDF computed exactly for the reaction of D meson decay into a vector meson $D^\pm \rightarrow K^*(892) + \ell^\pm + N$ is in good agreement with the PDF computed with the PYTHIA default matrix element for decays of D mesons (1), see figure 7.

The result, at least for the initial B and D mesons, can be summarized as follows. The parton level PYTHIA default matrix element (2) works well for a pseudoscalar meson 3-body decay into a pseudoscalar meson, a charged lepton and an HNL. The parton level PYTHIA default matrix element (1) works well for a pseudoscalar meson 3-body decay into a vector meson, a charged lepton and an HNL.

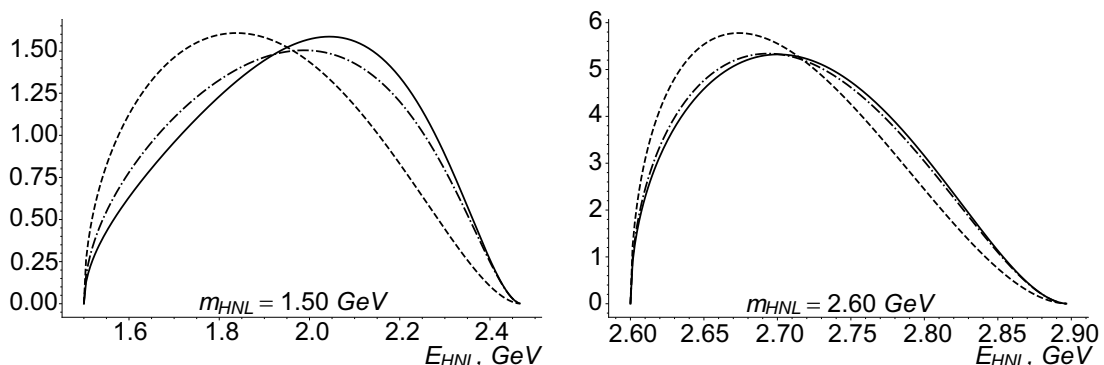


Figure 5: Probability density functions for the energy of HNLs (in the rest frame of the initial meson) produced in the reaction $B^\pm \rightarrow D^*(2007)^0 + \ell^\pm + N$ computed exactly (solid line), with the PYTHIA default matrix element for decays of B meson (2) (dashed line) and with the PYTHIA default matrix element for decays of D meson (1) (dot-dashed line).

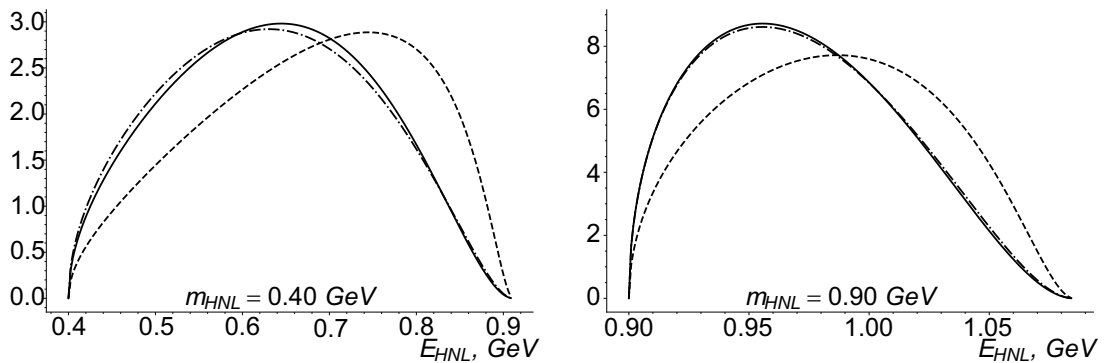


Figure 6: Probability density functions for the energy of HNLs (in the rest frame of the initial meson) produced in the reaction $D^\pm \rightarrow K^0 + \ell^\pm + N$ computed exactly (solid line) and with the PYTHIA default matrix element for decays of D meson (1) (dashed line) and with the PYTHIA default matrix element for decays of B meson (2) (dot-dashed line).

An intriguing question is how the sufficiently large difference in the PDFs will affect the quantities necessary for calculating the sensitivity region, namely ϵ_{geom} and P_{decay} . We consider this question in section 9 and section 10.

8 Distribution functions

Data *Data_h* for distribution of the produced h mesons (h stands for B or D mesons) in proton-target collisions (along axis z) in the SHiP experiment over the energy (E_h) and polar angle (θ_h) values were kindly provided by the SHiP collaboration. These data were obtained by using a tuned PYTHIA 6.4, see [68] for more details. In the following calculations, a data array with $a_B = 6.27 \cdot 10^5$ elements of type (E_B, θ_B) and a data array with $a_D = 10^6$ elements of type (E_D, θ_D) are used.

We use these data to calculate the distribution functions for the energy (E_N^{lab}) and the polar angle (θ_N^{lab}) of the produced HNLs in the laboratory frame with the help of Monte-Carlo simulation. Kinematic relations for HNLs between the laboratory and h meson's

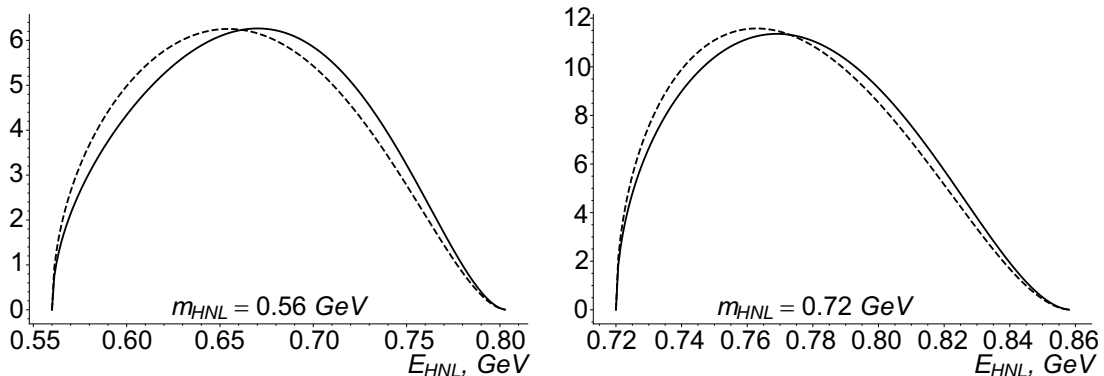


Figure 7: Probability density functions for the energy of HNLs (in the rest frame of the initial meson) produced in the reaction $D^\pm \rightarrow K^*(892) + \ell^\pm + N$ computed exactly (solid line) and with the PYTHIA default matrix element for decays of D meson (1) (dashed line).

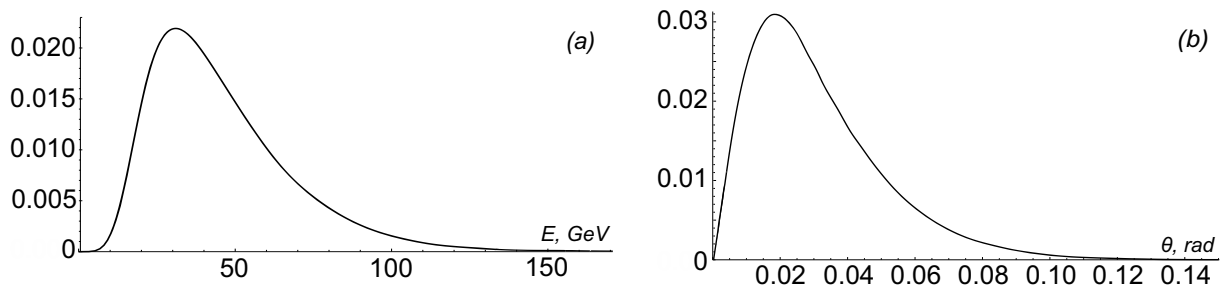


Figure 8: Probability density functions for energy (a) and polar angle (b) in the laboratory frame for HNLs with mass 2.6 GeV produced in the reaction $B^\pm \rightarrow D^*(2007)^0 + \ell^\pm + N$.

own reference frames are presented in appendix A. Corresponding relations contain dependence on two parameters of the h meson in the laboratory reference frame (the energy E_h and the polar angle θ_h) and four parameters of the HNL in the own reference frame of the h meson (the mass of the HNL m_N , the energy of the HNL E_N^{cm} , the polar and azimuth angles of the HNL $\theta_N^{cm}, \varphi_N^{cm}$).

It should be noted that in the h meson's own reference frame, the energy of the HNL is defined by the energy probability distribution function (17), but directions of motion of the produced HNL are equiprobable because of the isotropic property of the h meson decay. So we take these parameters ($y = \cos \theta_N^{cm}$ and φ_N^{cm}) with randomly chosen values. A set of values (E_h, θ_h) is taken from the elements of *Data h* with a serial number that is taken in a random way. Thus we receive data (*Data N*) in a form ($E_N^{lab}, \theta_N^{lab}$).

Using the obtained data, we can now derive probability density functions (PDF) and cumulative distribution functions (CDF) for energy and polar angle for HNLs and for the initial h mesons also. As an example, we present the PDFs for energy and polar angle (computed via the matrix element from section 6) in the laboratory reference frame for HNLs with mass 2.6 GeV produced in reaction $B^\pm \rightarrow D^*(2007)^0 + \ell^\pm + N$, see figure 8.

Using the definition of the median value as a value corresponding to the cumulative distribution function equal to 1/2, we get the median values of energy and polar angle for the initial B and D mesons produced in the SHiP experiment, namely $\overline{E_B} \simeq 80$ GeV, $\overline{\theta_B} \simeq 0.022$ and $\overline{E_D} \simeq 16.5$ GeV, $\overline{\theta_D} \simeq 0.022$.

For the produced HNLs the corresponding median values depend on their masses and the reaction of their production. As an example, for an HNL with mass 2.6 GeV produced in the reaction $B^- \rightarrow D^*(2007)^0 + e^- + N$, see figure 8, the median values of energy and polar angle in the laboratory reference frame are $\overline{E_N} \simeq 40$ GeV and $\overline{\theta_N} \simeq 0.026$.

9 Factor ϵ_{geom}

In this section we consider the probability of a produced HNL to move toward the detector (ϵ_{geom}). To do this, we have to find the probability of the polar angle θ_N^{lab} of the produced HNL to be less than the angular size of the detector e.g. for the SHiP experiment $\theta_{detector} = 0.028$. It is just the value of the cumulative distribution function ($F_{N,\theta}$) for the polar angle of the HNL in the laboratory frame

$$\epsilon_{geom}(m_N) = F_{N,\theta}(m_N) = \int_0^{\theta_{detector}} pdf(m_N, \theta) d\theta, \quad (42)$$

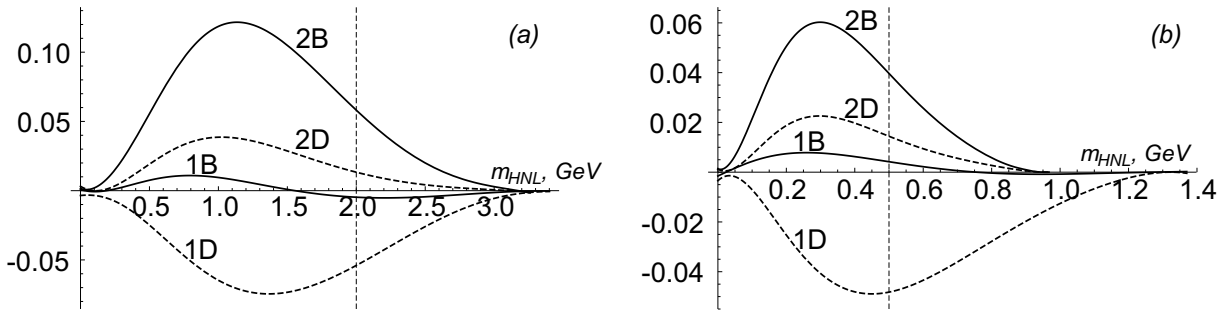


Figure 9: We present ratio $\frac{\epsilon_{geom}^{PYTH} - \epsilon_{geom}}{\epsilon_{geom}}$ for the produced HNLs. Figure (a) corresponds to the B meson decays (lines 1B and 1D: $B^\pm \rightarrow D^0 + \ell^\pm + N$, lines 2B and 2D: $B^\pm \rightarrow D^*(2007)^0 + \ell^\pm + N$). Figure (b) corresponds to the D meson decays (lines 1D and 1B: $D^\pm \rightarrow K^0 + \ell^\pm + N$, lines 2D and 2B: $D^\pm \rightarrow K^*(892) + \ell^\pm + N$). Dashed line corresponds to computations via the PYTHIA matrix element (1). Solid line corresponds to computations via the PYTHIA matrix element (2). We are only interested in the area to the right of the vertical dashed line.

where $pdf(m_N, \theta)$ is the PDF on polar angle θ of the HNL. Value of ϵ_{geom} depends on the mass of the HNL and the matrix element for its production.

The result of our computations can be presented in the following way. Factor ϵ_{geom} computed exactly (with the help of matrix elements presented in section 5 and section 6) for the reactions $B^\pm \rightarrow D^0 + \ell^\pm + N$ and $D^\pm \rightarrow K^*(892) + \ell^\pm + N$ is in good agreement (the relative difference is of order 1% – 2% in the area to the right of the vertical dashed line) with factor ϵ_{geom} computed with the help of the parton level PYTHIA default matrix elements for decays of B and D mesons correspondingly, see line 1B of figure 9(a) and line 2D of figure 9(b). But for the reactions $B^\pm \rightarrow D^*(2007)^0 + \ell^\pm + N$ and $D^\pm \rightarrow K^0 + \ell^\pm + N$ it is more preferable to use the parton level PYTHIA default matrix elements for decays of D and B mesons correspondingly, see line 2D of figure 9(a) and line 1B of figure 9(b). It should be noted that a similar situation was for computations of PDFs in section 7. We emphasize that in figure 9(b) the experimentally interesting area is $m_{HNL} \gtrsim 0.5$ GeV (to the right of the vertical dashed line) and in figure 9(a) it is $m_{HNL} \gtrsim 2$ GeV (to the right of the vertical dashed line), see section 1.

As one can see from figure 9 the probabilities of a produced HNL to move towards the detector coincide ($\epsilon_{geom}^{PYTH} = \epsilon_{geom}$) for an HNL with the maximum kinetically allowed value of the mass. This is how it should be. In the case when an HNL has the maximum value of mass, the initial hadron in its own reference frame decays into three motionless particles. All these particles in the laboratory frame will move in the direction of the initial meson regardless of the matrix element type.

10 Factor P_{decay}

The number of the produced HNLs that can be detected during the period of the SHIP operation is defined by (9). This relation allows us to find the region of parameters (m_N, U_α) , with which HNLs can be detected.

Behavior of the lower bound of this region for coupling constant (θ) can be estimated analytically. In this case arguments of the exponents in P_{decay} (10) are small and approx-

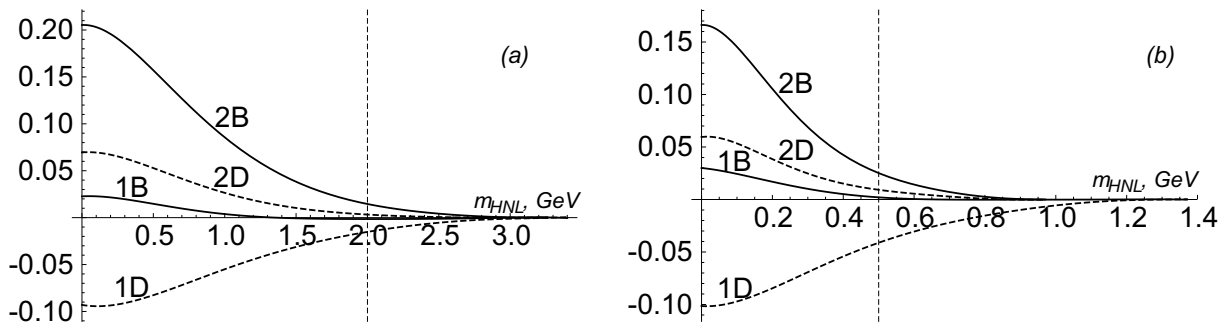


Figure 10: We present ratio $\frac{P^{PYTH} - P_{decay}}{P_{decay}}$ for the produced HNLs. Figure (a) corresponds to the B meson decays (lines 1B and 1D: $B^\pm \rightarrow D^0 + \ell^\pm + N$, lines 2B and 2D: $B^\pm \rightarrow D^*(2007)^0 + \ell^\pm + N$). Figure (b) corresponds to the D meson decays (lines 1D and 1B: $D^\pm \rightarrow K^0 + \ell^\pm + N$, lines 2D and 2B: $D^\pm \rightarrow K^*(892) + \ell^\pm + N$). Dashed line corresponds to computations via the PYTHIA matrix element (1). Solid line corresponds to computations via the PYTHIA matrix element (2). We are only interested in the area to the right of the vertical dashed line.

imation $e^x \simeq 1 + x$ can be used and we get

$$P_{decay} \approx \Delta L \cdot \Gamma \cdot X(E_N/m_N), \quad (43)$$

where $X(u) = (u^2 - 1)^{-1/2}$.

With the help of (43) we can easily obtain the ratio of P_{decay} computed for the exact matrix elements (see section 5 and section 6) and for the matrix elements in the PYTHIA approximation, see (1) and (2):

$$\frac{P_{decay}^{PYTH}}{P_{decay}} = \frac{\tilde{X}^{PYTH}(E_N/m_N)}{\tilde{X}(E_N/m_N)}, \quad (44)$$

where \tilde{X} is the median value of the corresponding function X . The median value of the function X was found by computing the median of the set of the X -function values produced by Monte Carlo simulations, see section 8.

The results of our computations are similar to the results of the analysis of the ϵ_{geom} factor. Factor P_{decay} computed exactly (with the help of the matrix elements presented in section 5) for the reactions $B^\pm \rightarrow D^0 + \ell^\pm + N$ is in good agreement (the relative difference is about 1% for $m_N \gtrsim 2$ GeV) with factor P_{decay} computed with the help of the parton level PYTHIA default matrix elements (2) for decays of B mesons, see line 1B of figure 10(a). Factor P_{decay} computed exactly (with the help of the matrix elements presented in section 6) for the reactions $D^\pm \rightarrow K^*(892) + \ell^\pm + N$ is in agreement (the relative difference less than 3% for $m_N \gtrsim 0.5$ GeV) with factor P_{decay} computed with the help of the parton level PYTHIA default matrix elements (1) for decays of D mesons, see line 2D of figure 10(b).

It should be noted that for the reactions $B^\pm \rightarrow D^*(2007)^0 + \ell^\pm + N$ and $D^\pm \rightarrow K^0 + \ell^\pm + N$ it is more preferable to use the parton level PYTHIA default matrix elements for decays of D and B mesons correspondingly, see line 2D of figure 10(a) and line 1B of figure 10(b). As in the case with ϵ_{geom} we are only interested in the area to the right of the vertical dashed line.

11 Conclusions

There are some indisputable phenomena that point to the fact that the SM has to be modified and complemented by a new particle (particles). We are sure that new physics exists, but we do not know where to search for it. There are many theoretical possibilities to modify the SM, namely by scalar, pseudoscalar, vector, pseudovector, or fermion particles of new physics. These particles may be substantially heavier than the energy scale of the present colliders. However, they may also be light (with mass less than the electroweak scale) and feebly interact with the SM particles.

In this paper, we consider the HNL extension of the SM. We analyzed the relevance of using the parton level PYTHIA default matrix elements without additional tuning for describing GeV-scale HNL production in the most important 3-body decays of B , D mesons that is a topical question for construction of the sensitivity region for the experimental search for HNLs. Our study was driven by the use of such an approximation in the SHiP collaboration paper [44]. We consider this question concerning the SHiP experiment, but our results are also applicable to other intensity frontier experiments.

Some general conclusions can now be drawn. The computations of the 3-body decays of τ leptons with HNL production in the PYTHIA approximation coincide with the exact computations, but the parton level PYTHIA default matrix elements for describing the 3-body decays of mesons are just similar to the matrix elements for free quark electroweak decays. Despite this, we have shown that this PYTHIA approximation has the right to be used for construction of the sensitivity region for the experimental search for HNLs, provided one uses the suitable parton level PYTHIA default matrix elements.

We consider the case of 3-body decays of B and D mesons into a light meson, an HNL and either an electron or a muon. These two cases of leptons in the final state are practically indistinguishable because of the small electron and muon masses as compared with the masses of mesons in the reactions. Reactions with τ leptons in the final state are either forbidden (for the decays of D mesons) or ineffective (as it was pointed in the Introduction HNL production from B meson decays can be neglected for HNLs with masses $m_N \lesssim 2$ GeV).

As it was shown in section 3, explicit form of matrix elements for HNL production in a 3-body decay affects factors ϵ_{geom} and P_{decay} (probabilities of the produced HNL to move toward the detector and to decay inside the vacuum tank before the detectors correspondingly) in the relation (9) that defines the sensitivity region of the intensity frontier experiments.

In section 9 and section 10 we conducted a detailed analysis of factors ϵ_{geom} and P_{decay} . Summing up the results of this analysis, one can conclude that for the description of HNL production in a 3-body decay of a pseudoscalar meson into another pseudoscalar meson ($B^\pm \rightarrow D^0 + \ell^\pm + N$ and $D^\pm \rightarrow K^0 + \ell^\pm + N$) the parton level PYTHIA matrix element (2) is better to use. For the description of HNL production in a 3-body decay of a pseudoscalar meson into a vector meson ($B^\pm \rightarrow D^*(2007)^0 + \ell^\pm + N$ and $D^\pm \rightarrow K^*(892) + \ell^\pm + N$) the parton level PYTHIA matrix element (1) is better to use.

Actually, it is more important to analyze the product $\epsilon_{geom} \cdot P_{decay}$, which is included in the relation (9) that defines the sensitivity region for HNLs. Considering other factors in (9) fixed, this allows us to obtain the total error of the quantity N_{det} , which directly defines the accuracy of the sensitivity region construction. We demonstrate the discrepancies for $\epsilon_{geom} \cdot P_{decay}$ in figure 11. We emphasize that in figure 11(b) the experimentally interesting area is $m_{HNL} \gtrsim 0.5$ GeV (region to the left of the vertical dashed line is almost completely closed by experiments [19, 42]) and in figure 11(a) the interesting area is $m_{HNL} \gtrsim 2$ GeV,

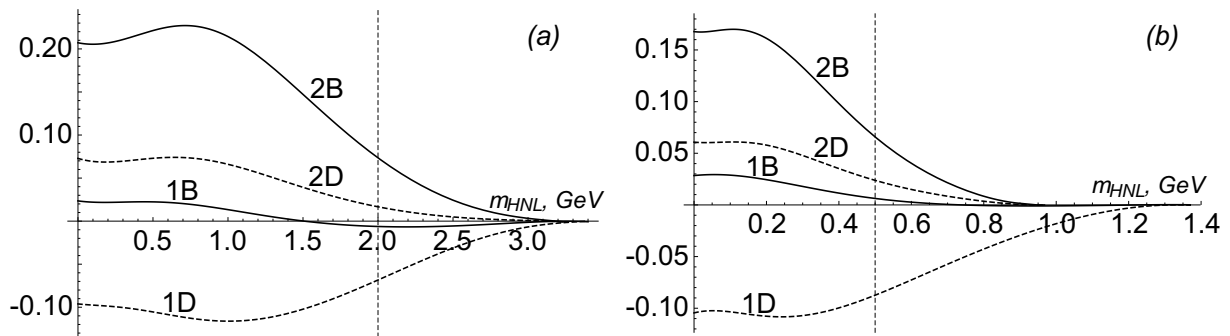


Figure 11: We present ratio $\frac{\epsilon_{geom}^{PYTHIA} P_{decay}^{PYTHIA} - \epsilon_{geom} P_{decay}}{\epsilon_{geom} P_{decay}}$ for HNLs produced in the 3-body decays of mesons for the default PYTHIA matrix elements. Figure (a) corresponds to the B meson decays (lines 1B and 1D: $B^\pm \rightarrow D^0 + \ell^\pm + N$, lines 2B and 2D: $B^\pm \rightarrow D^*(2007)^0 + \ell^\pm + N$). Figure (b) corresponds to the D meson decays (lines 1D and 1B: $D^\pm \rightarrow K^0 + \ell^\pm + N$, lines 2D and 2B: $D^\pm \rightarrow K^*(892) + \ell^\pm + N$). Dashed line corresponds to computations via the PYTHIA matrix element (1). Solid line corresponds to computations via the PYTHIA matrix element (2). We are only interested in the area to the right of the vertical dashed line.

where the production of HNLs in B mesons decays is effective, see section 1.

One can see that if we use default matrix element (2) for both the considered decays of B meson (into $D^*(2007)$ as well as into D^0), we get quite a large maximum discrepancy $\simeq 7.3\%$ for the reaction $B^\pm \rightarrow D^*(2007)^0 + \ell^\pm + N$, see line 2B of figure 11(a). Similarly, if we use default matrix element (1) for decays of D meson into K^0 as well as into $K^*(892)$ we get quite a large maximum discrepancy $\simeq 8.8\%$ for reaction $D^\pm \rightarrow K^0 + \ell^\pm + N$, see line 1D of figure 11(b). This is just the case implemented by the SHiP collaboration.

We come to the conclusion that if, for some reasons, under computations for HNL production in 3-body decays of mesons only default matrix elements are used, without additional tuning, it must be done in a more reasonable way. The most suitable choice of the parton level PYTHIA default matrix elements (1), (2) is as shown by lines 1B and 2D for figure 11(a) and figure 11(b). With this choice, one can get, among all the considered B and D meson decays, the smallest difference with the exact matrix element for the reaction $D^\pm \rightarrow K^0 + \ell^\pm + N$ (the relative difference less than 0.6%), while the largest irremovable difference is for the reaction $D^\pm \rightarrow K^*(892) + \ell^\pm + N$ (the relative difference less than 2.4%).

To summarize, it can be noted at least for the initial B and D mesons that the parton level PYTHIA default matrix element (2) works well for a pseudoscalar meson 3-body decay into a pseudoscalar meson, a charged lepton and an HNL. The parton level PYTHIA default matrix element (1) works well for a pseudoscalar meson 3-body decay into a vector meson, a charged lepton and an HNL. The interesting question of the possibility of generalizing this statement for other initial meson states requires further investigation.

It is important to note that the results of our research apply not only to physics beyond the Standard Model but also for the SM processes of semileptonic decays of mesons, see figure 11 at zero HNL mass.

In no case should our research be considered as a call to use only the parton level PYTHIA default matrix elements instead of accurate calculations using additional tuning for PYTHIA. We just checked the possibility and correctness of using the default matrix elements approach.

A Useful kinematic relations for the HNLs in the different reference frames

Let us consider an h meson with mass m_h and a given 4-momentum (E_h, \vec{p}_h) in the laboratory reference frame. Its velocity in this reference frame (the origin of coordinates is at the point of proton-target collisions, axis z is directed to the center of detector) is

$$\vec{V}_h^{lab} = |\vec{V}_h^{lab}| \vec{e}_h^{lab}, \quad (\text{A.1})$$

where

$$|\vec{V}_h^{lab}| = |\vec{p}_h| (m_h^2 + \vec{p}_h^2)^{-1/2}, \quad \vec{e}_h^{lab} = (\sin \theta_h \cos \varphi_h, \sin \theta_h \sin \varphi_h, \cos \theta_h). \quad (\text{A.2})$$

θ_h and φ_h are the polar and azimuth angles of the h meson's velocity vector in spherical coordinate system.

The absolute value of the HNL's velocity in the center-of-mass system of the produced particles (own reference frame of the initial h meson) is

$$\vec{V}_N^{cm} = |\vec{V}_N^{cm}| \vec{e}_N^{cm}, \quad (\text{A.3})$$

where

$$|\vec{V}_N^{cm}| = |\vec{p}_{N,cm}| (m_N^2 + \vec{p}_{N,cm}^2)^{-1/2}, \quad \vec{e}_N^{cm} = (\sin \theta_N^{cm} \cos \varphi_N^{cm}, \sin \theta_N^{cm} \sin \varphi_N^{cm}, \cos \theta_N^{cm}). \quad (\text{A.4})$$

θ_N^{cm} and φ_N^{cm} are the polar and azimuth angles of the HNL's velocity vector in the center-of-mass system. It should be noted that in the center-of-mass system of the produced particles the decay of the h meson is isotropic and the angles θ_N^{cm} and φ_N^{cm} can be arbitrary.

To find the value and the direction of the HNL's velocity in the laboratory reference frame we have to find the components of \vec{V}_N^{cm} that are parallel and perpendicular to the direction of \vec{V}_h^{lab} , namely $\vec{V}_{N,\parallel}^{cm}$ and $\vec{V}_{N,\perp}^{cm}$.

It's obvious that $\vec{V}_{N,\parallel}^{cm} = V_{N,\parallel}^{cm} \vec{e}_h^{lab}$, where

$$V_{N,\parallel}^{cm} = |\vec{V}_N^{cm}| \vec{e}_h^{lab} \cdot \vec{e}_N^{cm} = |\vec{V}_N^{cm}| (\sin \theta_N^{cm} \sin \theta_h \cos(\varphi_h - \varphi_N^{cm}) + \cos \theta_N^{cm} \cos \theta_h) \quad (\text{A.5})$$

is the projection of vector \vec{V}_N^{cm} on the direction \vec{e}_h^{lab} . Its value can be either positive or negative.

Consider now vector $\vec{V}_{N,\perp}^{cm} = |\vec{V}_{N,\perp}^{cm}| \vec{e}_{N,\perp}^{cm}$, where

$$|\vec{V}_{N,\perp}^{cm}| = |\vec{V}_N^{cm}| |\vec{e}_N^{cm} \times \vec{e}_h^{lab}|. \quad (\text{A.6})$$

Vector $\vec{V}_{N,\perp}^{cm}$ has to lie in the plane of vectors \vec{V}_N^{cm} and \vec{V}_h^{lab} . The equation of this plane is $\vec{n} \cdot (\vec{r} - \vec{r}_0) = 0$, where \vec{n} is the normal vector of the plane $\vec{n} = \vec{e}_N^{cm} \times \vec{e}_h^{lab}$ and $\vec{r} - \vec{r}_0$ is vector lying in the plane. Radii \vec{r} and \vec{r}_0 are meant to be taken with a base in the center of target. We put \vec{r}_0 (point of the h meson decay) to be a zero vector, because the distance between the point of production of meson and the point of its decay is very small compared with the distance from the target to the detector. As the vector \vec{r} we can use the unit vector of direction $\vec{e}_{N,\perp}^{cm}$.

Components of the unit vector $\vec{e}_{N,\perp}^{cm} = (\tilde{\alpha}, \tilde{\beta}, \tilde{\gamma})$ have to satisfy the following equations

$$\begin{cases} \vec{e}_h^{lab} \cdot \vec{e}_{N,\perp}^{cm} = \tilde{\alpha} \sin \theta_h \cos \varphi_h + \tilde{\beta} \sin \theta_h \sin \varphi_h + \tilde{\gamma} \cos \theta_h = 0, \\ n_x \tilde{\alpha} + n_y \tilde{\beta} + n_z \tilde{\gamma} = 0, \\ \tilde{\alpha}^2 + \tilde{\beta}^2 + \tilde{\gamma}^2 = 1. \end{cases} \quad (\text{A.7})$$

One can get the solution in the form $\vec{e}_{N,\perp}^{cm} = \vec{N}/|\vec{N}|$, where $\vec{N} = (\alpha, \beta, \gamma)$,

$$\begin{aligned} \alpha &= \cos \theta_N^{cm} \cos \theta_h \sin \theta_h \cos \varphi_h - \\ &\quad - \sin \theta_N^{cm} (\cos^2 \theta_h \cos \varphi_N^{cm} + \sin^2 \theta_h \sin(\varphi_h - \varphi_N^{cm}) \sin \varphi_h), \\ \beta &= \cos \theta_N^{cm} \cos \theta_h \sin \theta_h \sin \varphi_h - \\ &\quad - \sin \theta_N^{cm} (\cos^2 \theta_h \sin \varphi_N^{cm} - \sin^2 \theta_h \sin(\varphi_h - \varphi_N^{cm}) \cos \varphi_h), \\ \gamma &= \sin \theta_h (\cos \theta_h \sin \theta_N^{cm} \cos(\varphi_h - \varphi_N^{cm}) - \sin \theta_h \cos \theta_N^{cm}) \end{aligned} \quad (\text{A.8})$$

and the normalized coefficient $|\vec{N}|$ is equal to $|\vec{e}_N^{cm} \times \vec{e}_h^{lab}|$. The obtained solution has ambiguity, because the system of equations (A.7) is invariant under simultaneous change of sign of all the vector's components. This ambiguity can be removed under the following condition. If scalar product $\vec{N} \cdot \vec{V}_N^{cm}$ is positive the sign of vector \vec{N} is correct, otherwise the sign of vector \vec{N} has to be changed.

So, vector $\vec{V}_{N,\perp}^{cm}$ is simply defined as

$$\vec{V}_{N,\perp}^{cm} = \alpha |\vec{V}_{N,\perp}^{cm}| \vec{e}_{N,\perp}^{cm} = \alpha |\vec{V}_{N,\perp}^{cm}| \vec{N}/|\vec{N}|, \quad \alpha = \text{sgn}[\vec{N} \cdot \vec{e}_N^{cm}]. \quad (\text{A.9})$$

Now we can find the value and the direction of the HNL's velocity in the laboratory reference frame

$$V_{N,\parallel}^{lab} = \frac{|\vec{V}_h^{lab}| + V_{N,\parallel}^{cm}}{1 + V_{N,\parallel}^{cm} |\vec{V}_h^{lab}|}, \quad \vec{V}_{N,\parallel}^{lab} = V_{N,\parallel}^{lab} \vec{e}_h^{lab} \quad (\text{A.10})$$

$$|\vec{V}_\perp^{lab}| = |\vec{V}_{N,\perp}^{cm}| \frac{\sqrt{1 - |\vec{V}_h^{lab}|^2}}{1 + V_{N,\parallel}^{cm} |\vec{V}_h^{lab}|}, \quad \vec{V}_{N,\perp}^{lab} = \alpha |\vec{V}_N^{cm}| \vec{N}, \quad (\text{A.11})$$

$$|\vec{V}_N^{lab}| = \sqrt{|\vec{V}_{N,\parallel}^{lab}|^2 + |\vec{V}_{N,\perp}^{lab}|^2}. \quad (\text{A.12})$$

The components of the HNL's velocity vector \vec{V}_N^{lab} are

$$\begin{aligned} (\vec{V}_N^{lab})_x &= V_{N,\parallel}^{lab} (\vec{e}_h^{lab})_x + \alpha |\vec{V}_N^{cm}| (\vec{N})_x = |\vec{V}_N^{lab}| \sin \theta_N^{lab} \cos \varphi_N^{lab}, \\ (\vec{V}_N^{lab})_y &= V_{N,\parallel}^{lab} (\vec{e}_h^{lab})_y + \alpha |\vec{V}_N^{cm}| (\vec{N})_y = |\vec{V}_N^{lab}| \sin \theta_N^{lab} \sin \varphi_N^{lab}, \\ (\vec{V}_N^{lab})_z &= V_{N,\parallel}^{lab} (\vec{e}_h^{lab})_z + \alpha |\vec{V}_N^{cm}| (\vec{N})_z = |\vec{V}_N^{lab}| \cos \theta_N^{lab}, \end{aligned} \quad (\text{A.13})$$

where $(\vec{e}_h^{lab})_i$ and $(\vec{N})_i$ are the components of vectors (A.2), (A.8) and θ_N^{lab} , φ_N^{lab} are the angles of the HNL's velocity vector in the laboratory reference frame. The energy of the HNL in the laboratory reference frame is

$$E_N^{lab} = m_N \left(1 - |\vec{V}_N^{lab}|^2\right)^{-1/2}. \quad (\text{A.14})$$

In this paper we assume that the experiment facility has a cylindrical symmetry. Therefore, the azimuth angle of the h meson in the laboratory reference frame can be

set to zero ($\varphi_h = 0$). The energy E_N^{lab} and the direction of the HNL's velocity ($\theta_N^{lab}, \varphi_N^{lab}$) in the laboratory reference frame are defined only by six parameters: the energy E_h and the polar angle θ_h of the h meson in the laboratory reference frame, the two angles (θ_N^{cm} and φ_N^{cm}), the mass m_N and the energy E_N^{cm} of the produced HNL in the center-of-mass system of the produced particles (own reference frame of the h meson).

Acknowledgments

The authors are grateful to Alexey Boyarsky for statement of the problem and to Kyrylo Bondarenko for useful discussion and helpful comments.

References

- [1] Glashow S L 1961 Partial symmetries of weak interactions *Nucl. Phys.* **22** 579
- [2] Weinberg S 1967 A Model of Leptons *Phys. Rev. Lett.* **19** 1264
- [3] Salam A 1968 Weak and Electromagnetic Interactions *Proc. of 8th Nobel Symp.* ed. N Svartholm (Stockholm: Almquist and Wiksells) p 367
- [4] Bilenky S M 2014 Neutrino oscillations: brief history and present status *Proc. 22nd Int. Baldin Seminar on High Energy Physics Problems, Relativistic Nuclear Physics and Quantum Chromodynamics, (ISHEPP 2014): Dubna, Russia, September 15-20, 2014* (arXiv:1408.2864)
- [5] de Salas P F, Forero D V, Ternes C A, Tortola M and Valle J W F 2018 Status of neutrino oscillations 2018: first hint for normal mass ordering and improved CP sensitivity *Phys. Lett.* **B782** 633 (arXiv:1708.01186)
- [6] Peebles P J E 2013 Dark Matter *Proc. Nat. Acad. Sci.* **112** 2246 (arXiv:1305.6859)
- [7] Lukovic V, Cabella P and Vittorio N 2014 Dark matter in cosmology *Int. J. Mod. Phys.* **A29** 1443001 (arXiv:1411.3556)
- [8] Bertone G and Hooper D 2018 A History of Dark Matter *Rev. Mod. Phys.* (arXiv:1605.04909)
- [9] Brax Ph 2018 What makes the Universe accelerate? A review on what dark energy could be and how to test it *Rep. Prog. Phys.* **81** 016902
- [10] Steigman G 1976 Observational tests of antimatter cosmologies *Ann. Rev. Astron. Astrophys.* **14** 339
- [11] Strumia A and Vissani F 2010 Neutrino masses and mixings and... (arXiv:hep-ph/0606054)
- [12] Gorbunov D S and Rubakov V A 2011 *Introduction to the Theory of the Early Universe: Hot Big Bang Theory* World Scientific, Singapore, 2017
- [13] Gorkavenko V M 2019 Search for Hidden Particles in Intensity Frontier Experiment SHiP *Ukr. J. Phys.* **64** 689 (arXiv:1911.09206)

- [14] Beacham J *et al.* 2020 Physics Beyond Colliders at CERN: Beyond the Standard Model Working Group Report *J. Phys. G: Nucl. Part. Phys.* **47** 010501 (arXiv:1901.09966)
- [15] LBNE Collaboration, Adams C *et al.* The Long-Baseline Neutrino Experiment: Exploring Fundamental Symmetries of the Universe (arXiv:1307.7335)
- [16] SHiP Collaboration, Mermoud P 2017 Hidden sector searches with SHiP and NA62 *in 2017 Int. Workshop on Neutrinos from Accelerators (NuFact17) Uppsala University Main Building, Uppsala, Sweden, September 25-30, 2017* (arXiv:1712.01768)
- [17] NA62 Collaboration, Cortina Gil E *et al.* 2018 Search for heavy neutral lepton production in K^+ decays *Phys. Lett.* **B778** 137 (arXiv:1712.00297)
- [18] Drewes M, Hajer J, Klaric J and Lanfranchi G 2018 NA62 sensitivity to heavy neutral leptons in the low scale seesaw model *J. High Energ. Phys.* **2018** 105 (arXiv:1801.04207)
- [19] Alekhin S *et al.* 2016 A facility to Search for Hidden Particles at the CERN SPS: the SHiP physics case *Rep. Prog. Phys.* **79** 124201 (arXiv:1504.04855)
- [20] SHiP Collaboration, Anelli M *et al.* 2015 A facility to Search for Hidden Particles (SHiP) at the CERN SPS (arXiv:1504.04956)
- [21] Curtin D *et al.* 2019 Long-Lived Particles at the Energy Frontier: The MATHUSLA Physics Case *Rep. Prog. Phys.* **82** 116201
- [22] Patt B and Wilczek F 2006 Higgs-field portal into hidden sectors arXiv:hep-ph/0605188
- [23] Bezrukov F and Gorbunov D 2010 Light inflaton Hunter's Guide *JHEP* **05** 010
- [24] Boiarska I, Bondarenko K, Boyarsky F, Gorkavenko V, Ovchinnikov M 2019 Phenomenology of GeV-scale scalar portal *JHEP* **11** 162
- [25] Okun L B 1982 LIMITS OF ELECTRODYNAMICS: PARAPHOTONS? *Sov. Phys. JETP* **56** 502
- [26] Holdom B 1986 Two U(1)'s and Epsilon Charge Shifts *Phys. Lett. B* **166** 196
- [27] Langacker P 2009 The Physics of Heavy Z' Gauge Bosons *Rev. Mod. Phys.* **81** 1199
- [28] Peccei R D and Quinn H R 1977 CP Conservation in the Presence of Instantons *Phys. Rev. Lett* **38** 1440
- [29] Weinberg S 1978 A New Light Boson? *Phys. Rev. Lett.* **40** 223
- [30] Wilczek F 1978 Problem of Strong p and t Invariance in the Presence of Instantons *Phys. Rev. Lett.* **40** 279
- [31] Choi K, Im S H, Shin C S 2020 Recent progress in physics of axions or axion-like particles arXiv:2012.05029

- [32] Anastasopoulos P, Bianchi M, Dudas E, Kiritsis E 2006 Anomalies, anomalous U(1)'s and generalized Chern-Simons terms *JHEP* **11** 057
- [33] Antoniadis I, Boyarsky A, Espahbodi S, Ruchayskiy O, Wells J. D. 2010 Anomaly driven signatures of new invisible physics at the Large Hadron Collider *Nucl. Phys. B* **824** 296
- [34] Fukugita M and Yanagida T 2002 Resurrection of Grand Unified Theory Baryogenesis *Phys. Rev. Lett.* **89** 131602 (arXiv:hep-ph/0203194)
- [35] Akhmedov E K, Rubakov V A and Smirnov A Yu 1998 Baryogenesis via neutrino oscillations *Phys. Rev. Lett.* **81** 1359 (arXiv:hep-ph/9803255)
- [36] Asaka T and Shaposhnikov M 2005 The ν MSM, Dark Matter and Baryon Asymmetry of the Universe *Phys. Let. B* **620** 17 (arXiv:hep-ph/0505013)
- [37] Shaposhnikov M 2008 The ν MSM, leptonic asymmetries, and properties of singlet fermions *J. High Energ. Phys.* **08** 008 (arXiv:0804.4542)
- [38] Asaka T, Blanchet S and Shaposhnikov M 2005 The ν MSM, Dark Matter and Neutrino Masses *Phys. Let. B* **631** 151 (arXiv:hep-ph/0503065)
- [39] Boyarsky A, Ruchayskiy O and Shaposhnikov M 2009 The role of sterile neutrinos in cosmology and astrophysics *Ann. Rev. Nucl. Part. Sci.* **59** 191 (arXiv:0901.0011)
- [40] Boyarsky A, Ruchayskiy O, Iakubovskiy D and Franse J 2014 An unidentified line in X-ray spectra of the Andromeda galaxy and Perseus galaxy cluster *Phys. Rev. Lett.* **113** 251301 (arXiv:1402.4119)
- [41] Bulbul E, Markevitch M, Foster A, Smith R K, Loewenstein M and Randall S W 2014 Detection of An Unidentified Emission Line in the Stacked X-ray spectrum of Galaxy Clusters *Astrophys. J.* **13** 789 (arXiv:1402.2301)
- [42] Bondarenko K, Boyarsky A, Klaric J, Mikulenko O, Ruchayskiy O, Syvolap V, Timiryasov I 2021 An allowed window for heavy neutral leptons below the kaon mass (arXiv:2101.09255)
- [43] Bondarenko K, Boyarsky A, Gorbunov D and Ruchayskiy O 2018 Phenomenology of GeV-scale Heavy Neutral Leptons *J. High Energ. Phys.* **2018** 32 (arXiv:1805.08567)
- [44] Ahdida C, Albanese R *et al.* 2019 Sensitivity of the SHiP experiment to Heavy Neutral Leptons *J. High Energ. Phys.* **2019** 77 (arXiv:1811.00930)
- [45] Sjöstrand T, Mrenna S and Skands P Z 2008 A Brief Introduction to PYTHIA 8.1 *Comput. Phys. Commun.* **178** 852 (arXiv:0710.3820)
- [46] Sjöstrand T, Mrenna S and Skands P Z 2006 PYTHIA 6.4 Physics and Manual *J. High Energ. Phys.* **05** 026 (arXiv:hep-ph/0603175)
- [47] Bilenky S M and Petcov S T 1987 Massive neutrinos and neutrino oscillations *Rev. Mod. Phys.* **59** 671
- [48] E. Ma, Pathways to naturally small neutrino masses, *Phys. Rev. Lett.* **81** (1998) 1171, (arXiv:hep-ph/9805219)

- [49] Lazarides G, Shafi Q and Wetterich C 1981 Proton Lifetime and Fermion Masses in an $SO(10)$ Model *Nucl. Phys.* **B181** 287
- [50] Mohapatra R N and Senjanovic G 1981 Neutrino Masses and Mixings in Gauge Models with Spontaneous Parity Violation *Phys. Rev.* **D23** 165
- [51] Schechter J and Valle J W F 1980 Neutrino Masses in $SU(2) \times U(1)$ Theories *Phys. Rev.* **D22** 2227
- [52] Ma E and Sarkar U 1998 Neutrino masses and leptogenesis with heavy Higgs triplets *Phys. Rev. Lett.* **80** 5716 (arXiv:hep-ph/9802445)
- [53] Foot R, Lew H, He X G and Joshi G C 1989 Seesaw Neutrino Masses Induced by a Triplet of Leptons *Z. Phys.* **C44** 441
- [54] Mohapatra R N and Senjanovic G 1980 Neutrino Mass and Spontaneous Parity Violation *Phys. Rev. Lett.* **44** 912
- [55] Yanagida T 1980 Horizontal Symmetry and Masses of Neutrinos *Prog. Theor. Phys.* **64** 1103
- [56] Gorkavenko V M and Vilchynskiy S I 2010 Some constraints on the Yukawa parameters in the neutrino modification of the Standard Model (νMSM) and CP-violation *Eur. Phys. J. C* **70** 1091 (arXiv:0907.4484)
- [57] Ahdida C *et al.* 2019 The experimental facility for the Search for Hidden Particles at the CERN SPS *JINST* **14** P03025 (arXiv:1810.06880)
- [58] Tanabashi M *et al.* (Particle Data Group) 2018 and 2019 update *Phys. Rev. D* **98** 030001
- [59] Källén G 1964 *Elementary particle physics. Addison-Wesley series in advanced physics.* Addison-Wesley Pub. Co.
- [60] Bourely C, Lellouch L and Caprini I 2009 Model-independent description of $B \rightarrow \pi \ell \nu$ decays and a determination of $|V_{ub}|$ *Phys. Rev. D* **79** 013008 (arXiv:0807.2722)
2010 *Phys. Rev. D* **82** 099902 (erratum)
- [61] Aoki S *et al.* 2020 FLAG Review 2019 *Eur. Phys. J. C* **80** 113 (arXiv:1902.08191)
- [62] Na H, Bouchard C M, Lepage G P, Monahan C and Shigemitsu J 2015 $B \rightarrow D \ell \nu$ Form Factors at Non-Zero Recoil and Extraction of $|V_{cb}|$ *Phys. Rev. D* **92** 054510 (arXiv:1505.03925)
2016 *Phys. Rev. D* **93** 119906 (erratum)
- [63] Lubicz V, Riggio L, Salerno G, Simula S and Tarantino C 2017 Scalar and vector form factors of $D \rightarrow \pi(K) \ell \nu$ decays with $N_f = 2 + 1 + 1$ twisted fermions *Phys. Rev. D* **96** 054514 (arXiv:1706.03017)
2017 *Phys. Rev. D* **99** 099902 (erratum)
2019 *Phys. Rev. D* **100**, 079901 (erratum)
- [64] Ebert D, Faustov R N and Galkin V O 2007 Analysis of semileptonic B decays in the relativistic quark model *Phys. Rev. D* **75** 074008 (arXiv:hep-ph/0611307)

- [65] Faustov R N and Galkin V O 2014 Relativistic description of weak decays of Bs mesons *AIP Conf. Proc.* **1701** 050020 (arXiv:1411.7232)
- [66] Melikhov D and Stech B 2000 Weak form factors for heavy meson decays: An update *Phys. Rev. D* **62** 014006 (arXiv:hep-ph/0001113)
- [67] Mathur N, Padmanath M and Lewis R 2016 Charmed-Bottom mesons from Lattice QCD *PoS LATTICE2016* 100 (arXiv:1611.04085)
- [68] SHiP Collaboration, H. Dijkstra and T. Ruf 2015 *Heavy Flavour Cascade Production in a Beam Dump* CERN-SHiP-NOTE-2015-009